EARTHQUAKE ENGINEERING AND STRUCTURAL DYNAMICS, VOL. 26, 93–113 (1997)

MODAL ANALYSIS OF SOFT-SOIL SITES INCLUDING RADIATION DAMPING

J. X. ZHAO

Institute of Geological and Nuclear Sciences, Lower Hutt, New Zealand

SUMMARY

For the one-dimensional analysis of soft-soil layers on an elastic half-space, a general form of analytical solution is developed for converting radiation damping due to energy leaking back to the half-space into equivalent modal damping, allowing the modal analysis technique to be extended to a site where radiation damping has to be accounted for. Closed-form solutions for equivalent modal damping ratios and effective modal participation factors are developed for a single layer with a shear wave velocity distribution varying from constant to linearly increasing with depth. Compact and recursive forms of solutions for equivalent modal damping ratios are developed for a system with an arbitrary number of homogeneous layers on an elastic half-space. Comparisons with numerical solutions show that the modal solutions are accurate. The nominal frequency of a site, i.e. the inverse of four times the total shear wave travel time through the layers, is an important parameter for estimating the high mode frequencies. A parameter study shows that for the same impedance ratio of the bottom layer to the elastic half-space, a system of soil layers with an increasing soil rigidity with depth has, in general, larger peak modal amplifications at the ground surface than does a single homogeneous layer on an elastic half-space, while a system with a decreasing soil rigidity with depth has smaller modal peak amplifications.

KEY WORDS: modal analysis; radiation damping; equivalent damping ratio; site analysis

INTRODUCTION

It has been shown that site conditions can influence ground motions dramatically during an earthquake, as demonstrated by many recent event.[1,2] Much research has been carried out to investigate the modification of ground motions by soft-soil layers using one-dimensional (1-D)[3–9] or two-dimensional (2-D) models[10–13] for both linear and non-linear soils. There have been many successful applications of 1-D models to predict peak values of ground motions and response spectra of soft-soil sites where 2-D and 3-D effects have been recognized, though it is still debatable if a 1-D model can be used to predict the long duration of the ground motion of a soft-soil site.[11] One of the examples is the soft-soil site analysis for Mexcio City. Seed *et al.*[1] matched the recorded response spectra of soil sites using a nearby rock site record as the excitation and an equivalent linear approach[14] while Hadley *et al.*[15] predicted the ground surface responses of soil sites using the base motions generated from a 2-D model as the excitation to a 1-D non-linear model. Two-dimensional and 3-D effects of Mexico City were considered to be significant[11,16] but the effectiveness of 1-D models for engineering purposes was recognized.[11] For engineering applications, a 1-D model is still the most popular choice for site analysis because of its simplicity and easy interpretation of results. Two-dimensional models can also be used to obtain a simple relationship between the site response characteristics and the physical parameters of the soil layers.

For site amplification studies, two methods can be used. The frequency-domain approach assuming steady-state excitation, such as that in the SHAKE computer program,[14] uses an equivalent linear method and solves the dynamic equations of motion in the frequency domain. The alternative time-domain approach takes into account the transient part of the site response and solves the dynamic equations of motion in the time domain.[9] It has been shown by Sarma[17] that the transient part can be significant for certain cases, for

CCC 0098–8847/97/010093–21

Received 19 April 1996
Revised 23 July 1996

example, a site with a relatively long-period fundamental mode subjected to predominantly short-period earthquakes.

In both the time-domain and the frequency-domain analyses, modal analysis is usually preferred because fewer degrees of freedom are involved in the solution than in a numerical procedure for the direct time-domain analysis of the complete dynamic system.[18] An example of modal analysis in the frequency domain can be found from McVerry.[19]

When the half-space is assumed to be rigid, modal analysis can be used in both the time domain and the frequency domain. In the case where the flexibility of the half-space has to be taken into account, modal analysis cannot be used unless the radiation damping can be approximately converted into equivalent material damping.[20] For a single layer having a straight line variation in shear wave velocity with depth on a stiffer elastic half-space, a simple analytical model has been developed to account for the radiation damping for modal analysis.[20] Now a system with an arbitrary number of homogeneous layers is investigated. An analytical solution for equivalent damping ratios is derived by using the analytical modal shapes presented by Sarma[17] to account for the radiation damping. Radiation damping due to energy leaking back to the half-space is approximately converted into equivalent modal damping ratios and the modal analysis technique presented by Sarma[17] is then extended to solve the ground motions of such a soft-soil site. The calculation of the equivalent modal damping ratios for the radiation damping is very simple and can be carried out mode by mode starting from the first mode.

Understanding the effect of the half-space flexibility on the response of a soft-soil site, especially the frequency content of the ground surface response, is very important, in particular to the design of structures on the ground.[18,21] For a single layer with a straight line variation of shear wave velocity, it has been shown that the radiation damping attenuates low-frequency modes more than high-frequency modes.[6,17,20] For a multi-layer system, the effect of radiation damping may be quite different from that for a single layer.

In a previous study a linear hysteretic damping mechanism, which uses complex-valued stiffness, was assumed for the equivalent material damping to account for the energy radiation for simplicity.[20] The modelling procedure has now been improved so that either a viscous or a linear hysteretic damping mechanism can be assumed for the equivalent material damping.

For a single homogeneous layer, the modal frequencies of the site can be easily estimated. For a single layer with non-constant shear wave velocity variation with depth, or a system of an arbitrary number of homogeneous layers, numerical analysis usually has to be carried out to calculate the modal frequencies. In many engineering applications, four times the total travel time of a vertically propagating shear wave is usually taken as an estimate of the fundamental period of the site when numerical results are not available for a multi-layer system. It will be shown in this paper that such an estimate is actually not appropriate but is an important parameter for estimating the periods of high-frequency modes. A simple solution involving the travel time of the site is presented for estimating the high mode frequencies. This may be useful for an inverse problem, in which the variation of site shear wave velocity is unknown but the modal frequencies and other modal parameters can be estimated from available earthquake records.

Although modal analysis is generally used for linear response, applications to non-linear site response are possible if the radiation damping can be taken into account and appropriate use is made of the method developed for structural non-linear modal analysis.[22] Because analytical solutions for modal shapes, participation factors and equivalent modal damping ratios can be obtained at any level of the response, a modal analysis method for non-linear site analysis may be more efficient than the direct time-domain integration of the dynamic system equilibrium equations because only a small number of modes are required.

Parameter studies of the influence of radiation damping on the ground surface response of a multi-layer system are difficult to carry out because of the large number of parameters involved. However, some insights can be obtained from the investigation of a two-layer system and its conclusions can be generalized to a multi-layer system.

Material damping in the soil layers and in the half-space is assumed to be zero in the derivation of equivalent damping ratios in this paper, but the material damping of the soil layers can easily be taken into account by adding it to the equivalent damping ratios to obtain the total damping of the site.

Since the frequency-domain solution used in the SHAKE[14] program is widely interpreted as 'exact' and the finite element or finite difference methods in the time domain[9] are considered to be efficient, it may be argued as to why an approximate modal analysis should be used. The frequency-domain solution used in SHAKE is not 'exact' because the transient responses cannot be accounted for and the transient responses have been shown by Sarma[17] to be significant for certain cases. The numerical analysis procedure in the time domain[9] is not 'exact' either because of the spatial discretization errors associated with the finite element and finite difference methods (the high modal frequencies cannot be estimated accurately unless a very small element size is used). The modal analysis technique is not 'exact' because the radiation damping is approximated by modal damping, but is able to account for transient response and is free of spatial discretization errors. It will be shown that the error due to the approximation of radiation damping is small when the impedance ratio between the half-space and the bottom soil layer (see Figure 1) is reasonably large, for example greater than 3, and that the error diminishes with the increase of frequencies. In a case where transient and high-frequency responses are important while the impedance ratio is not small, the modal analysis presented in this paper would be a better candidate for the site amplification analysis than the above-mentioned existing methods. Compared with the numerical procedure using finite element or finite difference methods,[9] modal analysis can be very efficient because only a small number of modes is required and this is still true for non-linear analysis.[22] In a case where only peak response values of a soft-soil site are required from a given excitation, analysis based on the spectrum of the excitation[18] can be used to estimate approximately the peak response values in conjunction with the modal parameters given in this paper, without requiring numerical solutions for ground response time-history.

THE EQUIVALENT MATERIAL DAMPING OF A MULTI-LAYER SYSTEM

For a multi-layer system shown in Figure 1, with a constant shear wave velocity and a constant mass density in each layer and subjected to the excitation of steady-state and vertically propagating shear waves, it can be shown that the transfer function of the ground surface total displacement u_1 and the bedrock outcrop displacement u_0 has the general form (see Appendices II and III)

$$\frac{u_1}{u_0} = \frac{1}{R_T(\omega) + (i/p)\, I_T(\omega)} \tag{1}$$

where $R_T(\omega)$ and $I_T(\omega)$ are functions of parameters of the soil layers (and are both real if material damping does not exist), and i is the imaginary unit. The impedance ratio p is defined by

$$p = \frac{\rho_R \beta_R}{\rho_N \beta_N} \tag{2}$$

where ρ_R and β_R are, respectively, the mass density and the shear wave velocity of the half-space and ρ_N and β_N are the corresponding quantities in the bottom layer of the site. All other parameters of the site are defined in Figure 1. By setting $p = \infty$, the transfer function of the same multi-layer system on a rigid half-space can also be evaluated from equation (1). It can be shown that the modal frequencies of the undamped multi-layer system with a rigid base are the frequencies for which $R_T(\omega)$ in equation (1) equals zero. The proof for $R_T(\omega) = 0$ at modal frequencies can be found from Wolf[6] and Sarma[17] for the case of a single layer. For a multi-layer system, $R_T(\omega_j)$ for the jth modal circular frequency ω_j, which gives in equation (50a) in Appendix III of this paper, is the recursive form of the characteristic equations given in the appendices of Sarma[17] who has shown that the modal frequencies are the roots of the characteristic equations. $I_T(\omega)/p$ in equation (1) is the radiation damping term. Because the characteristic equation $R_T(\omega) = 0$ does not include the radiation damping term, the presence of radiation damping does not shift the resonance frequencies from the undamped modal frequency to the damped one, as noted by Sarma.[17] At the modal frequencies of the site, the real part of equation (1) is zero.

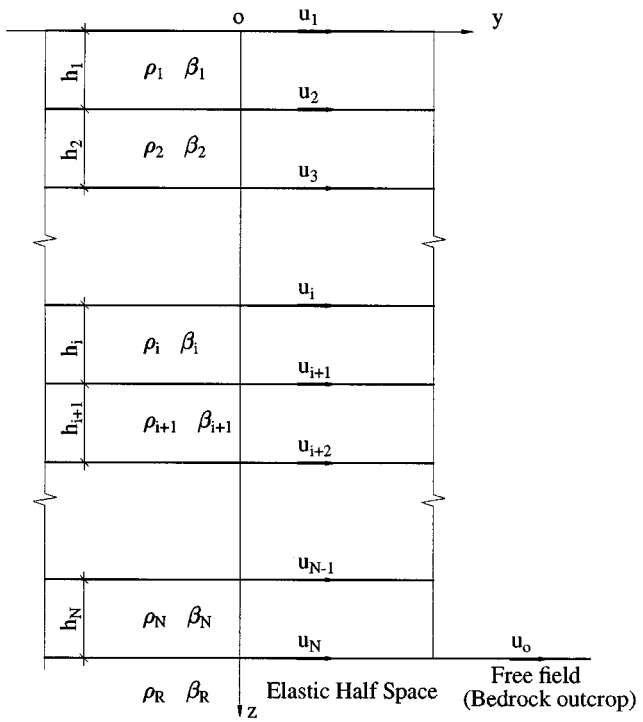

Figure 1. An arbitrary number of layers on an elastic half-space under the excitation of steady-state and vertically propagating in-plane shear waves. The thickness is denoted by h, mass density by ρ and shear wave velocity by β. The total displacement at each interface is denoted by u

For modal analysis, if a linear hysterestic damping mechanism can be assumed for the equivalent modal damping, the transfer function of the same layered system on a rigid half-space can be written as

$$\frac{u_1}{u_0} = \sum_{k=1}^{N_M} \frac{1 + 2i\xi_k^e}{1 - \omega^2/\omega_k^2 + 2i\xi_k^e} \mathscr{L}_k \tag{3}$$

where ω_k is the modal frequency, ξ_k^e is the equivalent material modal damping ratio, $\mathscr{L}_k$ is the Effective Modal Participation Factor (EMPF) at the ground surface for the kth mode and N_M is the total number of modes used in the analysis. At the undamped modal frequencies of the site, the real part of the transfer function given by equation (3) is much smaller than the imaginary part.

In order to convert the radiation damping into equivalent modal damping ratios, equation (1) has to be approximated by equation (3). Because both transfer functions given by equations (1) and (3) have peak values at the modal frequencies of the site ($R_T(\omega_k) = 0$), the matching of equations (1) and (3) is attempted at the modal frequencies only. Since the real part of equation (1) is zero and that of equation (3) is close to zero at the undamped modal frequencies, the two equations are approximately equal if the imaginary parts of the two equations are equal at $\omega = \omega_k$, i.e.

$$\frac{p}{I_T(\omega_k)} = \sum_{j=1}^{N_M} \frac{2\xi_j^e \, \omega_k^2/\omega_j^2}{[1 - \omega_k^2/\omega_j^2] + (2\xi_j^e)^2} \mathscr{L}_j \quad (k = 1, N_M) \tag{4}$$

When modal frequencies, EMPFs and $I_T(\omega_k)$ are known, equation (4) is sufficient to give all the damping ratios, but a large system of simultaneous equations must be solved. In this paper a simple approach is used instead. Numerical results show that at $\omega = \omega_k$, the contribution to the overall response from the modes with modal frequencies larger than ω_k is small, and therefore can be neglected. Thus for the first mode, the

equivalent damping ratio can be solved from

$$\xi_1^{\mathrm{e}} = \frac{\mathscr{L}_1 I_{\mathrm{T}}(\omega_1)}{2p} \tag{5}$$

and for the second or the higher mode,

$$\xi_k^{\mathrm{e}} = \frac{\mathscr{L}_k I_{\mathrm{T}}(\omega_k)}{2p\,\mu_k} \tag{6}$$

where μ_k is defined by (neglecting the products of damping ratios)

$$\mu_k = 1 - \frac{2\omega_k^2 I_{\mathrm{T}}(\omega_k)}{p} \sum_{j=1}^{k-1} \frac{\xi_j^{\mathrm{e}} \mathscr{L}_j}{\omega_j^2 (1 - \omega_k^2/\omega_j^2)^2} \tag{7}$$

Note that for a high-frequency mode, equivalent damping ratios are usually smaller than those for the low-frequency modes, and the frequency ratio ω_k/ω_j for $k > j$ is much larger than unity. Therefore for the fourth or higher mode, μ_k can be approximated from

$$\mu_k = 1 - \frac{2 I_{\mathrm{T}}(\omega_k)}{p\,\omega_k^2} \sum_{j=1}^{k-1} \xi_j^{\mathrm{e}} \mathscr{L}_j \omega_j^2 \tag{8}$$

If a viscous damping mechanism is assumed for the equivalent modal damping, the equivalent damping ratio for the first mode is identical to that given by equation (5), and for the second or higher mode the damping ratio is given by equation (6) but the modification factor μ_k is given by

$$\mu_k = 1 - \frac{2\omega_k^3 I_{\mathrm{T}}(\omega_k)}{p} \sum_{j=1}^{k-1} \frac{\xi_j^{\mathrm{e}} \mathscr{L}_j}{\omega_j^3 (1 - \omega_k^2/\omega_j^2)^2} \tag{9}$$

For the fourth and higher modes, μ_k can be calculated from

$$\mu_k = 1 - \frac{2\, I_{\mathrm{T}}(\omega_k)}{p\omega_k^3} \sum_{j=1}^{k-1} \xi_j^{\mathrm{e}} \mathscr{L}_j \omega_j^3 \tag{10}$$

If the material damping of the soil layers is not zero, the total modal damping ratio can be calculated for the kth mode from

$$\xi_k = \xi_k^{\mathrm{g}} + \xi_k^{\mathrm{e}} \tag{11}$$

where ξ_k^{g} is the modal damping ratio for the material damping of the soil layers.

It should be noted that the impedance ratio p has to be larger than about 2 to achieve a high degree of accuracy for the approximate solution. This is because the real part of equation (3) is too large to be neglected for small p, i.e. a large equivalent damping ratio.

For the multi-layer system shown in Figure 1, the characteristic equation for calculating the modal frequencies, and analytical recursive solutions for the EMPF $\mathscr{L}_k$ and $I_T(\omega_k)$, are given in Appendix III, and the equivalent modal damping ratios can be calculated from the equations given above. For a single-layer system having a specified variation in shear wave velocity with depth, the general form of the transfer function given in equation (1) and of the damping ratio in equation (6) can still be applied; however, as discussed below, there is a simple way of calculating the equivalent damping ratios for high-frequency modes.

EQUIVALENT MODAL DAMPING RATIOS FOR A SINGLE LAYER ON AN ELASTIC HALF-SPACE

For a single layer with a constant mass density and a constant shear wave velocity on an elastic half-space, using equations (5) where $I_{\mathrm{T}}(\omega)$ and $\mathscr{L}_k$ are given, respectively, in equations (56b) and (56c) in Appendix III,

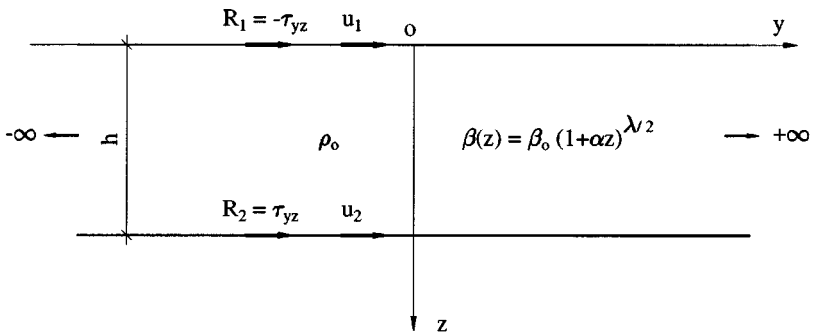

Figure 2. A single layer with a constant mass density ρ_0, a shear wave velocity variation function $\beta(z)$ and a thickness h under the excitation of steady-state and vertically propagating in-plane shear waves. The shear stress is denoted by τ_{yz} and displacement by u. Impedance ratios $p = \rho_R\beta_R/\rho_0\beta_0$ and $p_1 = \rho_R\beta_R/\rho_0\beta_0(1+\alpha)^{\lambda/2}$ are defined for this case

the equivalent damping ratio for the first mode is given by

$$\xi_1^e = \frac{2}{\pi p} \tag{12}$$

which is the same as given by Zhao.[20] It has been shown by Sarma[17] and Zhao[20] that the equivalent material damping ratio needed to account for the radiation damping is inversely proportional to the excitation frequency. Therefore, for the kth mode the equivalent modal damping ratio can be calculated from

$$\xi_k^e = \frac{2}{(2k-1)\pi p} \tag{13}$$

It can be shown that μ_k in equations (7)–(10) is very close to unity for this case and the equivalent modal damping ratios are approximately the same for both linear hysteretic and viscous damping mechanisms.

For a single layer with a constant mass density ρ_0 and a shear wave velocity variation with depth given by (see Figure 2)

$$\beta_L(z) = \beta_0\left(1+\alpha\frac{z}{h}\right)^{\lambda/2} \tag{14}$$

where β_0 is the shear wave velocity at the ground surface ($z = 0$), h is the thickness of the layer, α and λ are dimensionless parameters and $0 \leqslant \lambda < 2$, the equivalent damping ratio of the first mode can be calculated from

$$\xi_1^e = \left(\frac{\alpha\beta_0}{\omega_1 h\eta}\right)^{2\upsilon}\frac{(1+\alpha)^{1-3\lambda/2}}{p_1}\frac{1}{\mu}, \quad \mu = \frac{1}{1-J_\upsilon^2(\chi_{2,1})/J_{\upsilon-1}^2(\chi_{1,1})} \tag{15a, b}$$

where $p_1 = \rho_R\beta_R/\rho_0\beta_0(1+\alpha)^{\lambda/2}$, i.e. the impedance ratio of the half-space and the bottom surface of the layer, $J_\upsilon(\chi)$ is the Bessel's function of order υ, and η, υ, $\chi_{1,1}$ and $\chi_{2,1}$ are defined in Appendix I.

For the kth mode, as will be verified later, the equivalent modal damping ratio can be estimated from

$$\xi_k^e = \xi_1^e\frac{\omega_1}{\omega_k} \tag{16}$$

For a single layer with a constant mass density and a straight line variation of shear wave velocity with depth, corresponding to $\lambda = 2$ in equation (14), on an elastic half-space, the equivalent damping ratio of the first mode can be calculated from

$$\xi_1^e = \frac{\beta_0}{\omega_1 h}\frac{\alpha}{\ln(1+\alpha)}\frac{\mu}{p_1}, \quad \mu = \frac{\theta_1\sin^2\theta_1}{\theta_1-\sin\theta_1\cos\theta_1} \tag{17a, b}$$

where $p_1 = \rho_R \beta_R / \rho_0 \beta_0 (1 + \alpha)$ is the impedance ratio of the half-space and the bottom surface of the soil layer and θ_1 can be calculated from equation (38) of Appendix I by replacing ω with ω_1. Equation (5) has been used, where $I_T(\omega)$ and $\mathscr{L}_k$ are given, respectively, by equations (37b) and (39) in Appendix I. Equation (17a) is identical to that given by Zhao[20] but the modification factor μ has a different form from that given previously because of the different approximation adopted here. For the kth mode, the equivalent damping ratio can be calculated from equation (16), because the equivalent material damping is inversely proportional to the excitation frequency.[20]

COMPARISON OF ANALYTICAL SOLUTIONS WITH NUMERICAL RESULTS

The travel time T_0 for vertical incidence, and nominal frequency f_0 of a soil site can be defined, respectively, by

$$T_0 = \int_0^h \frac{\mathrm{d}z}{\beta(z)}, \qquad f_0 = \frac{1}{4T_0} \tag{18a, b}$$

where h is the total thickness of the soil layers and $\beta(z)$ is the variation function of the shear wave velocity with depth z. For a single layer with a constant shear wave velocity, f_0 is the first mode frequency of the layer. For a system with an arbitrary number of homogeneous layers or a system with arbitrary spatial variation of shear wave velocity, f_0 is an important parameter for estimating the frequencies of the high modes, as shown later, but is not necessarily a good approximation to the first mode frequency.

The case of a single layer with a shear wave velocity variation given by equation (14) above an elastic half-space is evaluated first. The transfer function between the ground surface displacement and the bedrock outcrop (the ground surface of the half-space in the absence of soil layers) displacement is evaluated by using the modal frequencies obtained from equation (32) (Appendix I), and the equivalent modal damping ratios and EMPFs from equations (15) and (35), respectively. The exact solution is calculated from equations (1) and (29). The same transfer function is also calculated using the SHAKE program[14] for which 15 homogeneous layers and an elastic half-space were used. The results are shown in Figure 3(a) and (b) for $\alpha = 3$, $\lambda = 1$, $\xi_g = 0{\cdot}05$ and $p_1 = 3$ and 4, respectively. Note that the modal solutions slightly overestimate the frequency of the first peak. This indicates that the modal frequencies of the equivalent site should be slightly reduced when radiation damping is accounted for by equivalent material damping, as noted by Zhao.[20] The agreement is very good. Differences between the phases of the transfer functions using the exact solution and the modal solution are very small and are not shown here.

The transfer function of a nine-layer soil system on an elastic half-space is shown in Figure 4. The material properties of the soil–layer system are given in Table I. The modal frequencies of the site, the equivalent damping ratios and the EMPFs are sloved from equations (48a) (with $R_T(\omega) = 0$), (6) and (50b), respectively. The same transfer function is also calculated using the SHAKE program. No material damping is considered so that the accuracy of the modal solutions at high frequencies can be assessed. Figure 4 shows that the modal solution matches the numerical solution very well. Some discrepancies occur in the frequency range between the first and second modes where the modal solutions slightly underestimate the transfer function compared with the results of the SHAKE program.

For the case of a single layer with a shear wave velocity variation given by equation (14), the modal frequencies normalized by the nominal frequency f_0 are shown in Figure 5(a). It can be clearly seen that the following equation can be used to estimate approximately the modal frequencies for the high-frequency modes for any practical value of α ($k \geqslant 2$):

$$\omega_k = 2\pi(2k - 1) f_0 \tag{19}$$

Equation (19) gives a very good estimate for even the third mode and the accuracy improves for the higher-frequency modes. Numerical results show that equation (19) also applies to a system with an arbitrary variation of shear wave velocity.

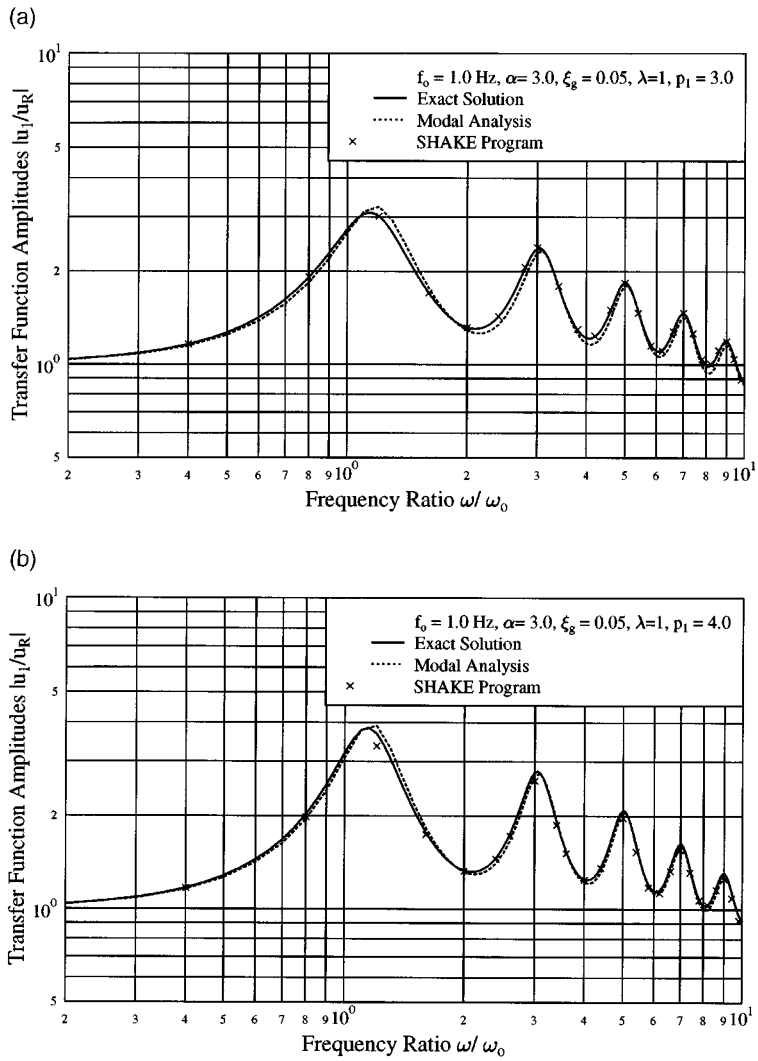

Figure 3. Transfer functions calculated for a single layer with shear wave velocity $\beta(z) = \beta_0(1 + \alpha z/h)^{\lambda/2}$. The modal solution matches the exact solution and the solution of the SHAKE program very well. (a) $p_1 = 3$, (*b*) $p_1 = 4$

To verify that the equivalent modal damping ratios are still inversely proportional to the modal frequencies for this case, the equivalent damping ratio of the first mode divided by the equivalent damping ratios of the higher modes calculated from equation (6) are compared with the corresponding inverse modal frequency ratios of Figure 5(b). It can be seen from Figure 5(b) that equivalent damping ratios are, approximately, inversely proportional to the modal frequency ratios, i.e. equation (16) will give good approximate values for the equivalent damping ratios of the high-frequency modes. Numerical results show that the equivalent modal damping ratios are not proportional to EMPFs, even though equation (6) seems to suggest that they are.

The EMPFs normalized by that of the first mode for a single layer with a variation in shear wave velocity given by equation (14) are shown in Figure 5(c). It can be seen that the EMPFs for high-frequency modes increase relative to that of the first mode with an increase of the shear wave velocity distribution factor α, indicating that energy associated with high-frequency modes is trapped near the ground surface for large values of α. On the other hand, for an elastic half-space with a given mass density and a given shear wave

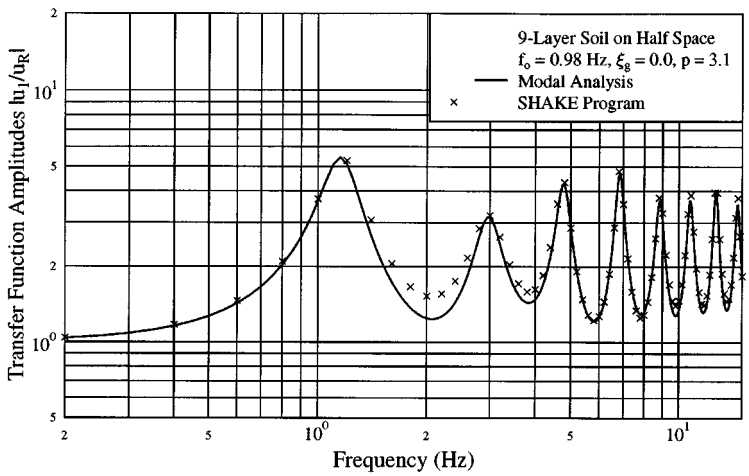

Figure 4. The transfer function of the modal solution calculated for a nine-layer system (Table I) by using the recursive form of the analytical solutions is compared with that of the SHAKE program. All the peak amplifications are well predicted by the modal solution

Table I. Material properties of the nine-layer system. The total travel time is 0·256 s

Layer no.	1	2	3	4	5	6	7	8	9
Mass density (kg/m^3)	1850	1800	1750	1750	1500	1550	1600	1600	1600
Thickness (m)	2·0	2·0	2·0	3·0	3·0	4·0	4·0	4·0	16·0
Velocity (m/s)	112	110	110	112	116	125	134	184	245
Half-space	Mass density $\rho_R = 2000$ kg/m^3			Shear wave velocity $\beta_R = 600$ m/s					

velocity, a large value of α means less velocity contrast at the interface between the layer and the half-space and more energy loss due to radiation damping.

Figure 5(d) shows the modal peak amplification ($\mathscr{L}_k/2\zeta_k^e$) for $p_1 = 3$ as a function of α. This would give the relative amplitude of contribution to the overall ground response from different modes. It can be seen that the modal peak amplification increases with increasing α and the modal peak amplification for high-frequency modes increases faster than for the first mode for a given impedance ratio of the layer and the half-space, indicating more high-frequency ground response for a larger value of α. It can also be seen that the contributions to the overall response from all the modes higher than the third are more or less the same even for large values of α. For a single homogeneous layer on a stiffer elastic half-space, the modal peak amplification equals p, the impedance ratio, and is the same for all modes as noted by Davis.[7]

MODAL PARAMETERS FOR A TWO-LAYER SYSTEM ON AN ELASTIC HALF-SPACE

Conducting a parameter study is difficult for a multi-layer system because of the large number of parameters. The following describes an analysis of a two-layer system on an elastic half-space, and some useful insights about the effect of radiation damping on the ground surface response are obtained.

The two-layer system is characterized by the first mode period of each layer, i.e. $T_A = 4h_1/\beta_1$ and $T_B = 4h_2/\beta_2$, the impedance ratio of the two layers, i.e. $r = \rho_1\beta_1/\rho_2\beta_2$, and the impedance ratio of the half-space and the bottom layer, i.e. $p = \rho_R\beta_R/\rho_2\beta_2$. Some of these parameters were used by Dobry *et al.*[5] for estimating the first mode period of such a site.

A case of $r = 0{\cdot}5$, i.e. with the top layer softer than the bottom layer, and $p = 3$ is investigated first. The modal frequencies normalized by the nominal frequency f_0 of the site are shown in Figure 6(a). It can be seen

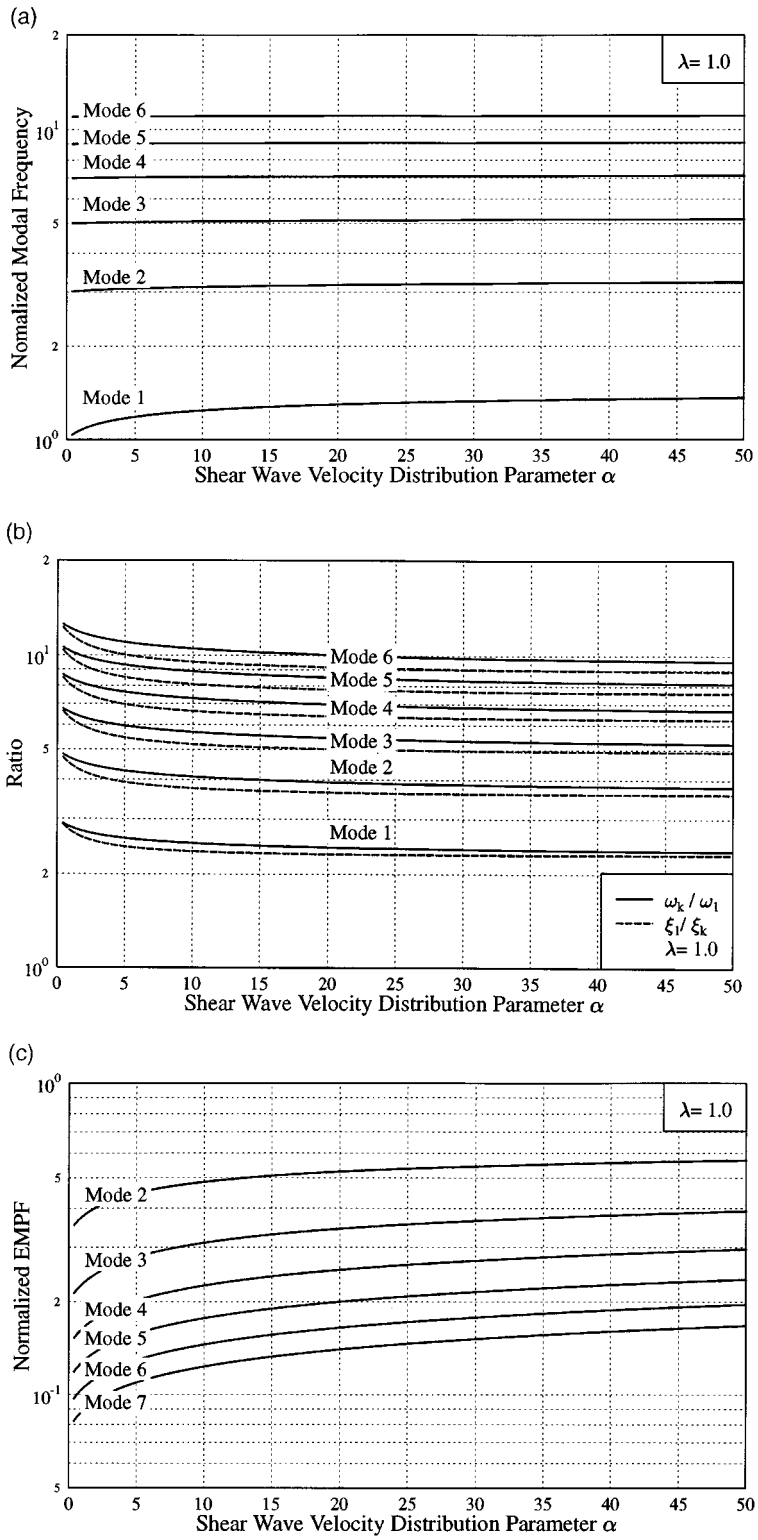

Figure 5. Modal parameters and modal peak amplification for a single layer with shear wave velocity $\beta(z) = \beta_0(1 + \alpha z/h)^{\lambda/2}$ $(0 \leqslant \lambda < 2)$. (a) Modal frequencies normalized by the nominal frequency f_0. Note that the first mode frequency is larger than f_0 but $(2k-1)f_0$ predicts the high mode frequencies very well. (b) The modal frequency ratios compared with the equivalent damping ratio of the first mode divided by that of a high-frequency mode. It can be seen that equivalent modal damping ratios are inversely proportional, approximately, to the modal frequencies. (c) The EMPF normalized by that of the first mode. Note that EMPF for high-frequency modes increase with the increase of α, indicating a tendency to trap high-frequency energy in the softer material near the top of the layer

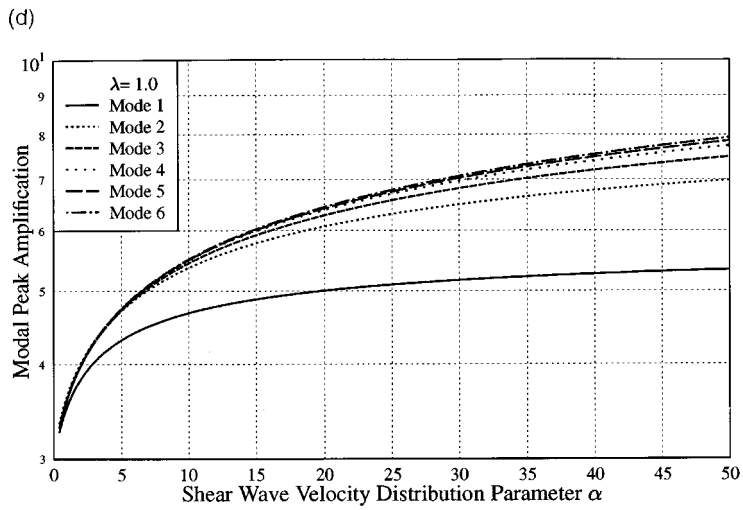

Figure 5. (d) Modal peak amplification ($\mathscr{L}_k/2\xi_k^e$) as functions of α. Note that modal peak amplification increases with the increase of α for all modes but increases faster for higher modes than for the first mode. For the fourth mode or higher, modal peak amplification takes almost the same value

that the first mode frequency is higher than f_0 and that equation (19) can be used to estimate the second or higher mode frequencies with good accuracy. The equivalent damping ratios are presented in Figure 6(b) as functions of T_B/T_A. It can be seen that the equivalent damping ratio of the first mode increases from about 10 per cent to about 20 per cent as the period ratio increases and is almost constant for a period ratio larger than 1·5. For the higher modes, the equivalent damping ratios vary within a range as the period ratio increases from 0·0 to 5·0 and the variation is more rapid for higher modes. For a small value of period ratio, all the equivalent damping ratios are close to r times those of a single homogeneous layer on an elastic half-space with the same impedance ratio of p. For a large-period ratio, all the equivalent modal damping ratios are more or less constant and are approaching those of a single homogeneous layer on an elastic half-space with the same impedance ratio of p. The variation of the EMPFs is shown in Figure 6(c) and is similar to that for equivalent damping ratios. At very small values of period ratio, the EMPFs have the same values as those of a single homogeneous layer. The EMPFs are generally larger than those for the case of a single homogeneous layer because energy is trapped in the top layer. The modal peak amplification, shown in Figure 6(d), varies between p = 3 to $p/r = 6$ and the peak amplification of the high-frequency modes is larger than that of the first mode for most values of the period ratio, indicating that high-frequency response may be dominant in such a site.

A second example with $r = 2{\cdot}0$, i.e. with the top layer stiffer than the bottom layer, and $p = 3$ is shown in Figure 7(a). The modal frequencies normalized by f_0 (see Figure 7(a)) indicate that the frequency of the first mode is always smaller than f_0. Equation (19) can also be used to estimate the mode frequencies of the higher modes. The equivalent damping ratios shown in Figure 7(b) demonstrate that the equivalent damping ratio of the first mode reduces from 40 per cent gradually to 20 per cent as the period ratio increases and that the equivalent damping ratios for higher modes are always much smaller than that of the first mode. The equivalent damping ratios are generally larger than those for the case of $r = 0{\cdot}5$ and $p = 3$, indicating that more energy is leaking back to the half-space because more upward propagating energy in the bottom layer is reflected downward at the layer interface and then the reflected waves are refracted back to the half-space. For a small value of period ratio, all the equivalent damping ratios equal r times those of a single homogeneous layer on an elastic half-space with the same impedance ratio of p, and for a large value of period ratio, all the equivalent damping ratios approach those of a single homogeneous layer. The EMPFs, shown in Figure 7(c), are generally smaller than those for the case of $r = 0{\cdot}5$ and are also smaller than those of a single homogeneous layer, indicating that energy is trapped in the bottom layer rather than the top layer.

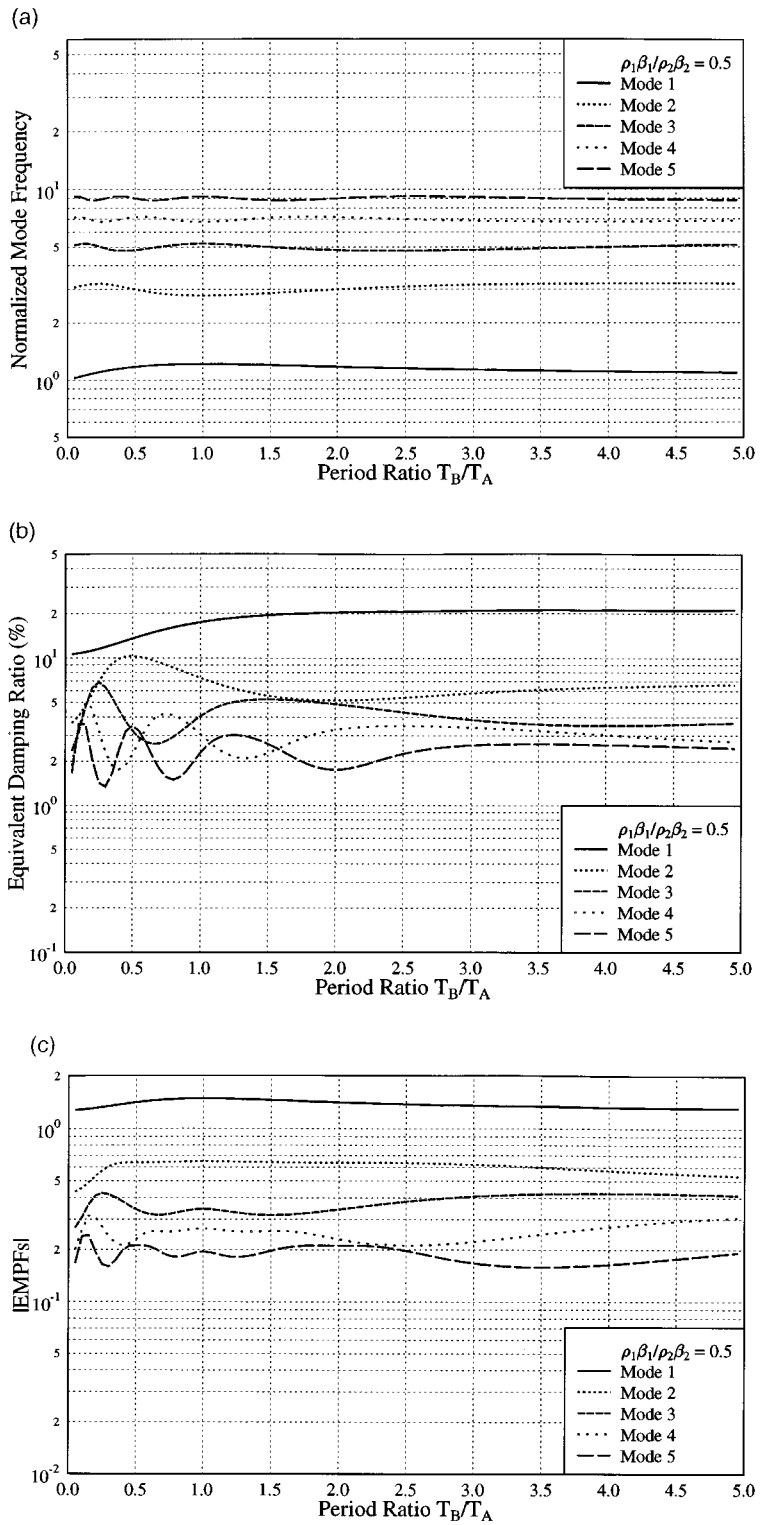

Figure 6. Modal parameters and modal peak amplification for a two-layer system with the top layer softer than the bottom layer and with an impedance ratio $p = 3$ at the interface with the half-space. (a) Modal frequencies normalized by the nominal frequency f_0. Note that the first mode frequency is larger than f_0 but $(2k - 1)f_0$ predicts the high mode frequencies very well. (b) The equivalent modal damping ratios. Note that for a small value of period ratio, and damping ratios are close to $r = \rho_1\beta_1/\rho_2\beta_2$ times those of the single homogeneous layer on a half-space with the same impedance ratio, and for a large value of period ratio all damping ratios approach those of the single homogeneous layer. (c) The effective modal participation factors. Note that EMPFs equal those of a single homogeneous layer for a very small value of period ratio

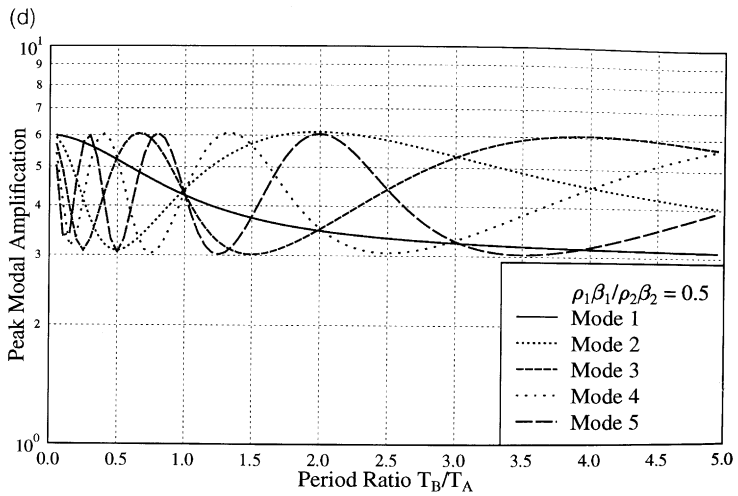

Figure 6. (d) Modal peak amplification. Note that modal peak amplification varies between p and p/r and the modal peak amplification of high-frequency modes is higher than that of the first mode for most values of period ratio

Not surprisingly, the modal peak amplification, shown in Figure 7(d), is much smaller than that for the case of $r = 0{\cdot}5$ and $p = 3$ because of the trapped energy in the bottom layer which leads to higher radiation damping for the same value of p. The model peak amplification varies between p and p/r and numerical results show that p and p/r are the limits of the modal peak amplification for any value of r and p. The first mode response becames dominant as the period ratio takes a larger value but the high-frequency responses can dominate the overall response of the site for a small value of period ratio.

The nominal frequency $f_0 = 0{\cdot}98$ is calculated for the nine-layer system for which the transfer function is presented in Figure 4 and the second or higher mode frequencies of the system can be very well estimated using equation (19).

It should be noted that material damping is not considered here for the parameter study. Material damping is more effective than radiation damping at attenuating the high-frequency response as noted by Davis,[7] and therefore the conclusion reached here that high-frequency mode response may dominate the overall response of a site may not apply when material damping is present.

Some insight on the ground surface response of a multi-layer site may be obtained from the parameter study carried out above. In general, the nominal frequency f_0 of a site is not an accurate estimate for the first mode frequency but is an important parameter for estimating the high mode frequencies. When the rigidity (product of mass density and shear wave velocity) of the soil increases with depth before reaching a stiffer elastic half-space, the first mode frequency is larger than the nominal frequency of the site calculated from the inverse of four times the travel time, and the ground surface responses for all modes are expected to be larger than those of a single homogeneous layer on an elastic half-space with the same first mode frequency and the same impedance ratio between the layer and the half-space. On the other hand, if the rigidity of the soil decreases with depth before reaching a stiffer elastic half-space, the first mode frequency is smaller than the nominal frequency of the site and the response at the ground surface is likely to be smaller than that of a site of single homogeneous layer on an elastic half-space with the same first mode frequency and the same impedance ratio.

For a layered soil site, the equivalent modal damping accounting for radiation damping is no longer inversely proportional to the excitation frequency as for a system with a single layer.

The impedance ratios $p \geqslant 2$ and $p_1 \geqslant 2$ are assumed for the general conclusion reached above. For a small value of p, some of the results presented by Davis[7] should be referred to, though the problem he addressed was a different one. He showed that a gradual change of shear modulus between the layer and the half-space

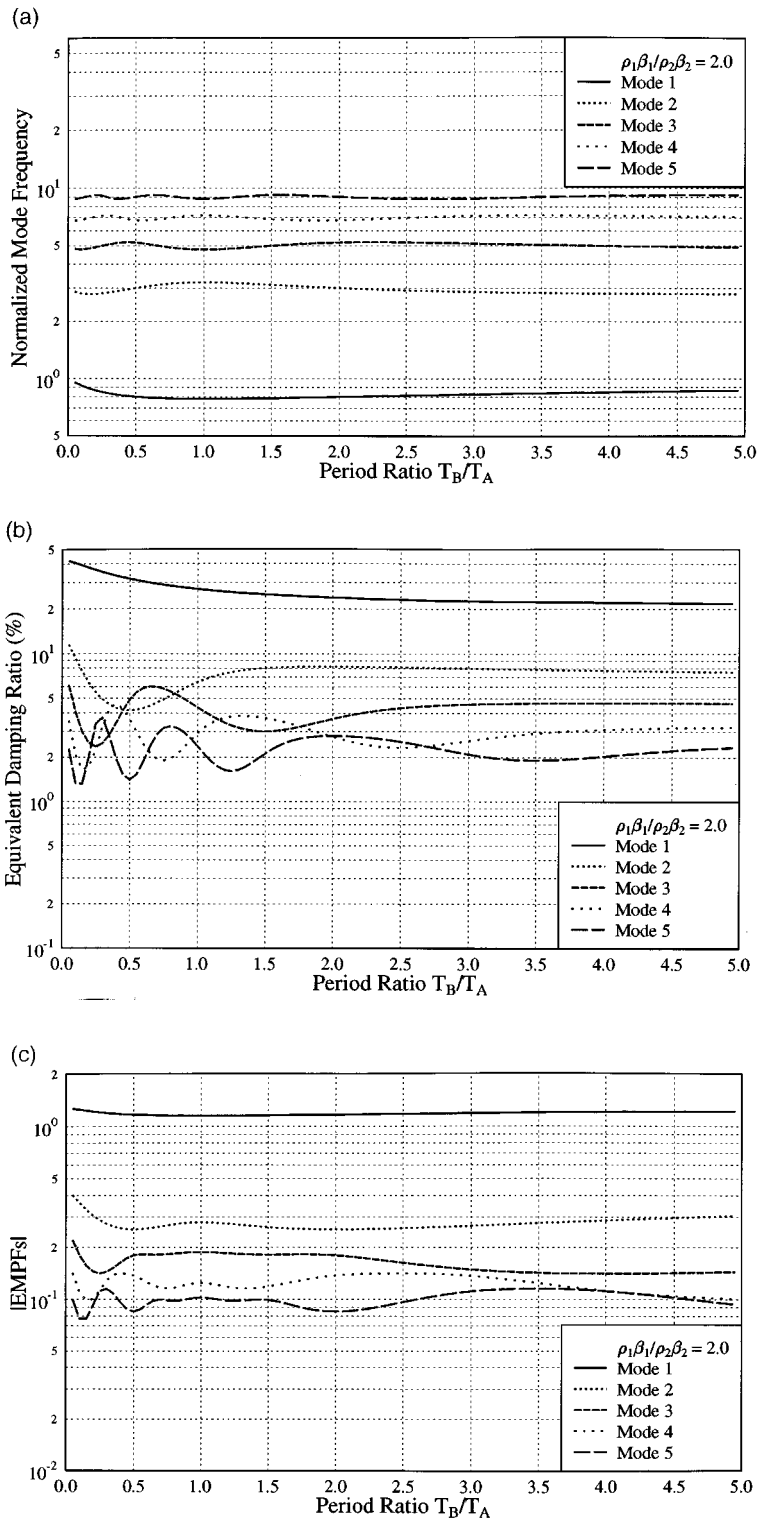

Figure 7. Modal parameters and modal peak amplification for a two-layer system with the top layer stiffer than the bottom layer and with an impedance ratio $p = 3$ at the interface with the half-space. (a) Modal frequencies normalized by the nominal frequency f_0. Note that the first mode frequency is smaller than f_0 but $(2k-1)f_0$ predicts the high mode frequencies very well. (b) The equivalent modal damping ratios. Note that similar variation as for Figure 6(b) but the equivalent damping ratio of the first mode is smaller than the corresponding one shown in Figure 6(b). (c) The effective modal participation factors. Note that EMPFs equal those of a single homogeneous layer for a very small value of period ratio and the variation of EMPFs with period ratio is smaller than that for equivalent damping ratios

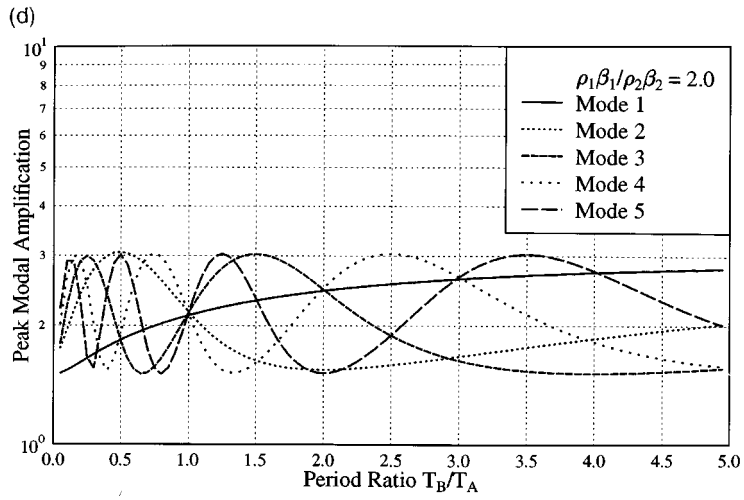

Figure 7. (d) Modal peak amplification. Note that modal peak amplification varies between p/r and p and the modal peak amplification of high-frequency modes is generally higher than that of the first mode for small values of period ratio

can reduce the site amplification at high frequencies by a large amount compared to that for a system of a single layer and a half-space separated by a perfect interface.

MAIN CONCLUSIONS

Analytical solutions for converting radiation damping to equivalent modal damping ratios are presented. The general analytical form of the solutions has been applied to both a system of a single layer having a particular variation of shear wave velocity with depth and an arbitrary number of homogeneous layers on an elastic half-space. The equivalent damping ratios can be assumed either linear hysterestic or viscous in nature.

For a multi-layer system, using the modal shapes presented by Sarma,[17] compact and recursive forms of analytical solutions for equivalent modal damping ratios are derived. Effective modal participation factors, modal shapes and characteristic equations are also presented in compact and recursive forms. The modal analysis method has thus been extended to a multi-layer system on an elastic half-space.

Analytical solutions for equivalent modal damping ratios and effective modal participation factors for a single layer having a shear wave velocity variation varying between constant and linearly increasing with depth are developed.

The results of modal analyses using the analytical solutions for modal frequencies, equivalent modal damping ratios and effective modal participation factors are shown to have acceptable accuracy compared with numerical solutions.

It has been shown that the nominal frequency of a site, i.e. the inverse of four times the total travel time of the soil layers, is an important parameter for estimating high mode frequencies. A simple equation for estimating high mode frequencies is presented and its accuracy is well within the requirement for engineering applications. The nominal frequency is, however, not a very good estimate for the first mode frequency of the site.

A parameter study is carried out for systems of a single layer and two layers on an elastic half-space. It has been shown that if the soil rigidity (product of soil mass density and shear wave velocity) increases with depth, the first mode frequency is larger than the nominal site frequency and the ratio of the second mode frequency to that of the first mode is smaller than 3. It has been shown that if the soil rigidity decreases with depth, the first mode frequency is smaller than the nominal site frequency and the ratio of the second mode

frequency to that of the first mode is larger than 3. This result may be useful in dealing with an inverse problem, where the modal frequencies can be estimated from earthquake records and ambient vibration measurements. It has also been shown that for the same impedance ratio between the bottom layer and the elastic half-space, a system of soil layers having an increasing soil rigidity with depth has, in general, larger peak modal amplifications at the ground surface than does a single homogeneous layer on an elastic half-space, while a system having a decreasing soil rigidity with depth has smaller modal peak amplifications.

The analytical modal solutions may be used for non-linear site analysis in which modal shapes, modal frequencies, equivalent modal damping ratios and effective modal participation factors can be calculated for a particular time step as in the non-linear modal analysis used for structures. Better accuracy than that from the finite difference and finite element methods may be achieved because the errors of spatial discretization inherited in those methods do not exist.

APPENDIX I

Single layer with continuous variation of shear wave velocities

For a site with a single horizontal soil layer, an analytical solution can be obtained only for a certain variation of shear wave velocity with depth.[4] A special case considered here is a single layer having a shear wave velocity variation described by equation (14) (shown in Figure 2). Under the excitation of steady-state vertically propagating shear waves, the governing differential equation of motion can be written as

$$\frac{\mathrm{d}^2u}{\mathrm{d}z^2} + \frac{\alpha\lambda}{h+\alpha z}\frac{\mathrm{d}u}{\mathrm{d}z} + \frac{\omega^2}{\beta_0^2}\left(1+\alpha\frac{z}{h}\right)^{-\lambda} u = 0 \tag{20}$$

where u is the displacement amplitude in the frequency domain.

For the case of $0 \leqslant \lambda \leqslant 2$, the complete solution of equation (20) is given by

$$u(\chi) = \chi^{\upsilon}[A\,J_{\upsilon}(\chi) + B\,Y_{\upsilon}(\chi)] \tag{21}$$

where A and B are constants, J_{υ} and Y_{υ} are, respectively, Besel's and Weber's functions of order υ and

$$\chi = \frac{\eta\omega}{\gamma}\left(1+\alpha\frac{z}{h}\right)^{1/\eta}, \quad \gamma = \alpha\frac{\beta_0}{h}, \quad \eta = \frac{2}{2-\lambda}, \quad \upsilon = 1-\frac{\eta}{2} \tag{22a–d}$$

The shear stress in the soil can be written as

$$\tau_{yz} = \frac{\alpha\rho_0\beta_0^2}{\eta h}\left(\frac{\eta\omega}{\gamma}\right)^{2-\eta}\chi^{\upsilon+\eta-1}\,[A\,J_{\upsilon-1}(\chi) + B\,Y_{\upsilon-1}(\chi)] \tag{23}$$

Setting the displacement $u(z) = u_1$ at $z = 0$ and $u(z) = u_2$ at $z = h$, it follows that

$$\begin{Bmatrix} u_1 \\ u_2 \end{Bmatrix} = \begin{bmatrix} \chi_1^{\upsilon}J_{\upsilon}(\chi_1) & \chi_1^{\upsilon}Y_{\upsilon}(\chi_1) \\ \chi_2^{\upsilon}J_{\upsilon}(\chi_2) & \chi_2^{\upsilon}Y_{\upsilon}(\chi_2) \end{bmatrix} \begin{Bmatrix} A \\ B \end{Bmatrix} \tag{24}$$

where

$$\chi_1 = \frac{\eta\omega}{\gamma}, \quad \chi_2 = \chi_1(1+\alpha)^{1/\eta} \tag{25a, b}$$

Setting shear stress $R_1 = -\tau_{yz}(z)$ at $z = 0$ and $R_2 = \tau_{yz}$ at $z = h$, it follows that

$$\begin{Bmatrix} R_1 \\ R_2 \end{Bmatrix} = \frac{\alpha\rho_0\beta_0^2}{\eta h}\left(\frac{\eta\omega}{\gamma}\right)^{2-\eta}\begin{bmatrix} -\chi_1^{\upsilon+\eta-1}J_{\upsilon-1}(\chi_1) & -\chi_2^{\upsilon+\eta-1}Y_{\upsilon-1}(\chi_1) \\ \chi_2^{\upsilon+\eta-1}J_{\upsilon-1}(\chi_2) & \chi_2^{\upsilon+\eta-1}Y_{\upsilon-1}(\chi_2) \end{bmatrix} \begin{Bmatrix} A \\ B \end{Bmatrix} \tag{26}$$

Solving for the constants A and B from equation (24), the stresses and the displacements of the layer are related by

$$\begin{Bmatrix} R_1 \\ R_2 \end{Bmatrix} = \frac{\alpha \rho_0 \beta_0}{S_Q} \begin{bmatrix} S_{11} & S_{12} \\ S_{21} & S_{22} \end{bmatrix} \begin{Bmatrix} u_1 \\ u_2 \end{Bmatrix} \tag{27}$$

where

$$S_{11} = \chi_1^{\eta-1} [Y_{\upsilon-1}(\chi_1) J_\upsilon(\chi_2) - J_{\upsilon-1}(\chi_1) Y_\upsilon(\chi_2)] \tag{28a}$$

$$S_{12} = S_{21} = -\frac{2}{\pi} (\chi_1 \chi_2)^{-\upsilon} \tag{28b}$$

$$S_{22} = \chi_2^{\eta-1} [Y_{\upsilon-1}(\chi_2) J_\upsilon(\chi_1) - J_{\upsilon-1}(\chi_2) Y_\upsilon(\chi_1)] \tag{28c}$$

$$S_Q = [J_\upsilon(\chi_1) Y_\upsilon(\chi_2) - J_\upsilon(\chi_2) Y_\upsilon(\chi_1)] \left(\frac{\eta\omega}{\gamma}\right)^{\eta-1} \tag{28d}$$

Using the direct stiffness matrix approach of Wolf,[6] it can be shown that the transfer function relating the total ground surface displacement u_1 to the bedrock outcrop displacement u_0 is given by equation (1) where

$$R_T(\omega) = -\frac{S_{11}}{S_{12}}, \quad I_T(\omega) = \frac{S_{11} S_{22} - S_{12} S_{21}}{S_Q S_{12}} \tag{29a, b}$$

Using the free surface boundary condition ($\tau_{yz} = 0$ at $z = 0$) the kth modal shape of the layer can be solved from equations (21) and (23) as

$$u_k(\chi_k) = \chi^\upsilon [J_\upsilon(\chi_k) Y_{\upsilon-1}(\chi_{1,k}) - Y_\upsilon(\chi_k) J_{\upsilon-1}(\chi_{1,k})] \tag{30}$$

where

$$\chi_k = \frac{\eta\omega_k}{\gamma} \left(1 + \alpha \frac{z}{h}\right)^{1/\eta}, \quad \chi_{1,k} = \frac{\eta\omega_k}{\gamma} \tag{31a, b}$$

Using the zero displacement boundary condition at $z = h$, the kth modal frequency ω_k can be solved from

$$J_\upsilon(\chi_{2,k}) Y_{\upsilon-1}(\chi_{1,k}) - J_{\upsilon-1}(\chi_{1,k}) Y_\upsilon(\chi_{2,k}) = 0 \tag{32}$$

where

$$\chi_{2,k} = \frac{\eta\omega_k}{\gamma} (1 + \alpha)^{1/\eta} \tag{33}$$

The effective modal participation factor $\mathscr{L}_k$ of the kth mode can be derived from

$$\mathscr{L}_k = u_k(\chi_{1,k}) \frac{\int_0^h u_k(\chi_k)\, dz}{\int_0^h u_k^2(\chi_k)\, dz} \tag{34}$$

Substituting equation (30) into equation (34), the kth effective modal participation factor can be derived as

$$\mathscr{L}_k = 2\chi_{1,k}^{-1} (1 + \alpha)^{-\upsilon/\eta} \frac{J_{\upsilon-1}(\chi_{1,k})}{J_\upsilon(\chi_{2,k})} \frac{1}{J_{\upsilon-1}^2(\chi_{1,k})/J_\upsilon^2(\chi_{2,k}) - 1} \tag{35}$$

Note that in equation (28a) $S_{11} = 0$ at $\omega = \omega_k$ and then using equation (32) and the special properties of Bessel's and Weber's functions[23] it follows that

$$S_Q(\omega_k) = \frac{2}{\pi} \left(\frac{\eta\omega_k}{\gamma}\right)^{\eta-2} \frac{J_\upsilon(\chi_{2,k})}{J_{\upsilon-1}(\chi_{1,k})}, \quad I_T(\omega_k) = \chi_{1,k}^{1-\upsilon} \chi_{2,k}^{-\upsilon} \frac{J_{\upsilon-1}(\chi_{1,k})}{J_\upsilon(\chi_{2,k})} \tag{36a, b}$$

For $\lambda = 2$, corresponding to a single layer with a straight line variation in shear wave velocity, the solutions are presented by Zhao,[20] and $R_T(\omega)$ and $I_T(\omega)$ are given by

$$R_T(\omega) = \frac{2m\cos\theta + \sin\theta}{2\,m\sqrt{1+\alpha}}, \quad I_T(\omega) = \frac{\omega\, h\sqrt{1+\alpha}}{\alpha\beta_0\, m}\sin\theta \tag{37a, b}$$

where

$$\theta = m\ln(1+\alpha), \quad m = \sqrt{\left(\frac{\omega h}{\alpha\beta_0}\right)^2 - 0{\cdot}25} \tag{38a, b}$$

The effective modal participation factor for the kth mode is given by[20]

$$\mathscr{L}_k = 2\left[\frac{\alpha\beta_0\theta_k}{h\omega_k\ln(1+\alpha)}\right]^2 \frac{\sqrt{1+\alpha}\,\sin\theta_k}{\theta_k - \sin\theta_k\cos\theta_k} \tag{39}$$

where θ_k is calculated from equation (38) replacing ω with ω_k.

Only the main results and some of the intermediate results are presented here because of the limited length of this paper. All equations given above apply to the layer with a flexible base except for equations (32)–(34) which apply only to the case of a rigid base. When the equivalent modal damping ratios are used, modal frequencies and effective modal participation factors from equations (33) and (34), respectively, still apply to the case of a flexible base.

APPENDIX II

A two-layer system

For a two layer system, taking $N = 2$ in Figure 1 in which each layer has a constant mass density and a constant shear wave velocity, under the excitation of steady-state and vertically propagating shear waves, the discretized dynamic equilibrium equation of motion can be written as[6]

$$\begin{bmatrix} \alpha_1\cot\gamma_1 & -\dfrac{\alpha_1}{\sin\gamma_1} & 0 \\ -\dfrac{\alpha_1}{\sin\gamma_1} & \alpha_1\cot\gamma_1 + \alpha_2\cot\gamma_2 & -\dfrac{\alpha_2}{\sin\gamma_2} \\ 0 & -\dfrac{\alpha_2}{\sin\gamma_2} & \alpha_2\cot\gamma_2 + \mathrm{i}\alpha_R \end{bmatrix} \begin{Bmatrix} u_1 \\ u_2 \\ u_3 \end{Bmatrix} = \begin{Bmatrix} 0 \\ 0 \\ \mathrm{i}\alpha_R u_0 \end{Bmatrix} \tag{40}$$

where

$$\alpha_1 = \beta_1\rho_1, \quad \alpha_2 = \beta_2\rho_2, \quad \alpha_R = \beta_R\rho_R \tag{41a–c}$$

$$\gamma_1 = \omega\frac{h_1}{\beta_1}, \quad \gamma_2 = \omega\frac{h_2}{\beta_2} \tag{41d, e}$$

The displacement u_1 in equation (40) is the ground surface displacement, u_2 is the displacement at the interface of the two layers and u_3 is the displacement at the interface between the bottom layer and the half-space.

It can be seen from equation (40) that

$$u_2 = u_1\cos\gamma_1 \tag{42}$$

The following parameters can be defined:

$$\theta_{2,1} = \gamma_1 + \gamma_2, \quad \theta_{2,2} = \gamma_1 - \gamma_2 \tag{43a, b}$$

$$Q_{2,1} = 0{\cdot}5\left(1 + \frac{\rho_1\beta_1}{\rho_2\beta_2}\right), \quad Q_{2,2} = 0{\cdot}5\left(1 - \frac{\rho_1\beta_1}{\rho_2\beta_2}\right) \tag{43c, d}$$

$$p = \frac{\rho_2\beta_2}{\rho_R\beta_R} \tag{43e}$$

Substituting equations (42) and (43) into equation (40) and eliminating u_2 from the system equations, it follows that

$$\frac{\cos\gamma_1}{\sin\gamma_2}\begin{bmatrix} Q_{2,1}\cos\theta_{2,1} + Q_{2,2}\cos\theta_{2,2} & -1 \\ -1 & \dfrac{\cos\gamma_2}{\cos\gamma_1} + \mathrm{i}p\,\dfrac{\sin\gamma_2}{\cos\gamma_1} \end{bmatrix}\begin{Bmatrix} u_1 \\ u_3 \end{Bmatrix} = \begin{Bmatrix} 0 \\ \mathrm{i}pu_0 \end{Bmatrix} \tag{44}$$

The transfer function between the displacement u_1 on the ground surface to that of the bedrock outcrop u_0 is given by equation (1) where

$$R_T(\omega) = Q_{2,1}\cos\theta_{2,1} + Q_{2,2}\cos\theta_{2,2}, \quad I_T(\omega) = Q_{2,1}\sin\theta_{2,1} - Q_{2,2}\sin\theta_{2,2} \tag{45}$$

The kth effective modal participation factor is given by

$$\mathscr{L}_k = \frac{2}{Q_{2,1}\theta_{2,1,k}\sin\theta_{2,1,k} + Q_{2,2}\theta_{2,2,k}\sin\theta_{2,2,k},} \tag{46}$$

where

$$\theta_{2,1,k} = \omega_k\left(\frac{h_1}{\beta_1} + \frac{h_2}{\beta_2}\right), \quad \theta_{2,2,k} = \omega_k\left(\frac{h_1}{\beta_1} - \frac{h_2}{\beta_2}\right) \tag{47a, b}$$

APPENDIX III

For a system with an arbitrary number of layers

For a system with an arbitrary number of homogeneous layers, as shown in Figure 1, using the same approach as for the two-layer system to eliminate all the interface displacements, a recursive form of the transfer function between the total displacements at the ground surface to that of the bedrock outcrop can be solved. For a system with i layers, the following general form can be derived:

$$R_T(\omega) = \sum_{j=1}^{N_i}\left[Q_{i,2j-1}\cos(\omega T_{i,2j-1}) + Q_{i,2j}\cos(\omega T_{i,2j})\right] \tag{48a}$$

$$I_T(\omega) = \sum_{j=1}^{N_i}\left[Q_{i,2j-1}\sin(\omega T_{i,2j-1}) - Q_{i,2j}\sin(\omega T_{i,2j})\right] \tag{48b}$$

where

$$Q_{i,2j-1} = \tfrac{1}{2}Q_{i-1,j}\left[1 + (-1)^{j+1}\,\frac{\rho_{i-1}\beta_{i-1}}{\rho_i\beta_i}\right] \tag{49a}$$

$$Q_{i,2j} = \tfrac{1}{2}Q_{i-1,j}\left[1 - (-1)^{j+1}\,\frac{\rho_{i-1}\beta_{i-1}}{\rho_i\beta_i}\right] \tag{49b}$$

$$T_{i,2j-1} = T_{i-1,j} + \frac{h_i}{\beta_i} \tag{49c}$$

$$T_{i,2j} = T_{i-1,j} - \frac{h_i}{\beta_i} \tag{49d}$$

$$N_i = 2^{i-2} \tag{49e}$$

The characteristic equation and the effective modal participation factor for the kth mode can be written as

$$R_{\mathrm{T}}(\omega_k) = \sum_{j=1}^{N_i} [Q_{i,2j-1} \cos(\theta_{i,2j-1,k}) + Q_{i,2j} \cos(\theta_{i,2j,k})] \tag{50a}$$

$$\mathscr{L}_k = \frac{2}{\sum_{j=1}^{N_i} [Q_{i,2j-1}\theta_{i,2j-1,k} \sin(\theta_{i,2j-1,k}) + Q_{i,2j}\theta_{i,2j,k} \sin(\theta_{i,2j,k})]} \tag{50b}$$

where

$$\theta_{i,2j-1,k} = \omega_k T_{i,2j-1}, \quad \theta_{i,2j,k} = \omega_k T_{i,2j} \tag{51a, b}$$

The kth modal shape for the top layer in a system with the total number of layers equal to i can be written as

$$\phi_{k,1}(z) = \cos\frac{z}{\beta_1} \tag{52}$$

and for the jth layer

$$\phi_{k,j}(z) = \sum_{n=1}^{N_j} \left\{ Q_{j,2n-1} \cos\left[\omega_k \left(T_{j-1,2n-1} + \frac{z - \bar{h}_{j-1}}{\beta_j}\right)\right] + Q_{j,2n} \cos\left[\omega_k \left(T_{j-1,2n} - \frac{z - \bar{h}_{j-1}}{\beta_j}\right)\right]\right\} \tag{53}$$

where $N_j = 2^{(j-2)}$, $j = 2, i$ and

$$\bar{h}_{j-1} = \sum_{n=1}^{j-1} h_n \tag{54}$$

For the case of a single layer where $i = 1$, following parameters are defined:

$$Q_{1,1} = 1, \quad T_{1,1} = \frac{h_1}{\beta_1}, \quad \theta_{1,1,k} = \omega_k T_{1,1} \tag{55a–c}$$

and the corresponding characteristic equation and the effective modal participation factor for the kth mode can be written as

$$R_T(\omega_k) = Q_{1,1} \cos(\theta_{1,1,k}) \tag{56a}$$

$$I_T(\omega_k) = Q_{1,1} \sin(\theta_{1,1,k}) \tag{56b}$$

$$\mathscr{L}_k = \frac{2}{Q_{1,1}\theta_{1,1,k} \sin(\theta_{1,1,k})} \tag{56c}$$

The modal shapes given in equations (52) and (53) and $R_T(\omega)$ given in equation (48a) are the compact and recursive versions of those developed by Sarma.[17]

For the case of a two-layer system, all the parameters are given in Appendix II.

ACKNOWLEDGEMENT

The author wishes to thank Drs. G. H. McVerry, R. A. Benites, W. J. Cousins and R. O. Davis for their review of the manuscript and Professor G.B. Warburton and an anonymous reviewer for their constructive suggestions. The research reported here was supported by the New Zealand Foundation for Research Science and Technology under contact CO5506.

REFERENCES

1. H. B. Seed, M. P. Romo, J. Sun, A. Jaime and J. Lysmer, 'Relationships between soil conditions and earthquake ground motions in Mexico city in the earthquake of Sept. 19, 1985', *Report No. UCB/EERC-87/15*, Earthquake Engineering Research Centre, University of California, Berkeley, 1987.
2. L. Benuska, 'Local site effects on strong ground motion and damage—Loma Prieta earthquake reconnaissance report', *Earthquake spectra* (Suppl.) **6**, 106–113 (1990).
3. N. N. Ambraseys, 'A note on the response of an elastic overburden of varying rigidity to an arbitrary ground motion', *Bull. seism. soc. Am.* **49**, 211–220 (1959).
4. I. M. Idriss and H. B. Seed, 'Seismic response of horizontal soil layers', *J. soil mech. found. div. ASCE* **94**, 1003–1031 (1968).
5. R. Dobry, I. Oweis and A. Urzua, 'Simplified procedures for estimating the fundamental period of a soil profile', *Bull. seism. soc. Am.* **66**, 1293–1321 (1976).
6. J. P. Wolf, *Dynamic Soil–Structure Interaction*, Prentice-Hall, Englewood Cliffs, NJ, 1985.
7. R. Davis, 'Effects of weathering on site response', *Earthquake eng. struct. dyn.* **25**, 301–309 (1995).
8. N. C. Tsai and G. W. Housner, 'Calculation of surface motions of a layered half space', *Bull. seism. soc. Am.* **60**, 1625–1651 (1970).
9. W. B. Joyner and A. T. F. Chen, 'Calculation of nonlinear ground responses in earthquakes', *Bull. seism. soc. Am.* **65**, 1315–1336 (1975).
10. P. -Y. Bard and J. Gariel, 'The seismic responses of two-dimensional sedimentary deposits with large vertical velocity gradients', *Bull. seism. soc. Am.* **76**, 343–346 (1986).
11. F. J. Chávez-García and P. Bard, 'Site effects in Mexico City eight years after the September 1985 Michoacan earthquakes', *Soil dyn. earthquake eng.* **13**, 229–247 (1994).
12. W. B. Joyner 'A method for calculating nonlinear seismic response in two dimensions', *Bull. seism. soc. Am.* **65**, 1337–1357 (1975).
13. J. Marsh, T. J. Larkin, A. J. Haines and R. A. Benites, 'Comparison of linear and nonlinear seismic responses of two-dimensional alluvial basins', *Bull. seism. soc. Am.* **85**, 874–889 (1995).
14. P. B. Schnabel and J. Lysmer, 'SHAKE — a computer program for earthquake response analysis of horizontally layered sites', *Report No. UCB/EERC-72/12,* Earthquake Engineering Research Centre, University of California, Berkeley, 1972.
15. P. K. Hadley, A. Askar and A. S. Cakmak, 'Subsoil geology and soil amplification in Mexico Valley', *Soil dyn. earthquake eng.* **10**, 101–109 (1991).
16. F. J. Sánchez-Sesma, L. E. Pérez-Rocha and E. Reinoso, 'Ground motion in Mexico city during the April 25, 1989 Guerro earthquarke', *Teconophysics* **218**, 127–140 (1993).
17. S. K. Sarma, 'Analytical solution to the seismic response to visco-elastic soil layers', *Géotechnique* **44**, 265–275 (1994).
18. R. W. Clough and J. Penzien, *Dynamics of Structures*, McGraw-Hill, New York, 1975.
19. G. H. McVerry, 'Structural identification in the frequency domain', *Earthquake eng. struct. dyn.* **8**, 161–180 (1980).
20. J. X. Zhao, 'Estimating modal parameters for a simple soft-soil site having a linear distribution of shear wave velocity with depth', *Earthquake eng. struct. dyn.* **25**, 163–178 (1996).
21. D. J. Dowrick, *Earthquake Resistant Design for Engineers and Architects*, 2nd edn, Wiley, New York, 1987.
22. P. Léger and S. Dussault, 'Non-linear seismic response analysis using vector superposition methods', *Earthquake eng. struct. dyn.* **21**, 163–176 (1992).
23. N. W. McLachlan, in E. B. Moullin, D. R. Pye and R. V. Southwell (eds), *Bessel Functions for Engineering*, The Oxford Engineering Science Series, Oxford University Press, London: Humphrey Milford, 1934.